International Journal of Mechanical Sciences 128-129 (2017) 572–582

Contents lists available at ScienceDirect

International Journal of Mechanical Sciences

journal homepage: www.elsevier.com/locate/ijmecsci

Frequency spectra of nonlocal Timoshenko beams and an effective method of determining nonlocal effect

Yin Zhang *[a,b]

[a] State Key Laboratory of Nonlinear Mechanics (LNM), Institute of Mechanics, Chinese Academy of Sciences, Beijing 100190, China
[b] School of Engineering Science, University of Chinese Academy of Sciences, Beijing 100049, China

ARTICLE INFO

Article history:
Received 25 January 2017
Received in revised form
26 April 2017
Accepted 16 May 2017
Available online 29 May 2017

Keywords:
Nonlocal effects
Timoshenko beam
Resonant frequency
Frequency spectrum

ABSTRACT

Three critical frequencies independent of boundary conditions together with a critical length, which determine the vibration behaviors of a nonlocal Timoshenko beam, are identified. Unlike a local Timoshenko beam which has two frequency spectra, a nonlocal Timoshenko beam may have two frequency spectra or one frequency spectrum depending on the nonlocal effect. The eigenfrequencies of the higher modes of a nonlocal Timoshenko beam, irrespective of its boundary conditions, are shown to asymptotically approach one critical frequency, which is mainly determined by the nonlocal effect and beam material properties. This asymptotic behavior is proposed as a new and reliable way to determine the nonlocal effect. The nonlocal effect is also shown to determine whether a special vibration mode called thickness shear vibration can occur.

1. Introduction

Compared with the Euler–Bernoulli beam model, the Timoshenko beam model [1,2] incorporates both the rotatory inertia and shear effects, which better characterizes the beam deformation. An interesting issue of two frequency spectra on the Timoshenko beam model was first brought up by Traill-Nash and Collar [3], which induced heated debates [4–9]. There is a critical frequency associated with the thickness shear vibration mode [4,8,10], which divides the frequency domain into two zones: the first frequency spectrum (frequency smaller than that of thickness shear vibration) and the second frequency spectrum (frequency larger than that of thickness shear vibration). For Traill-Nash and Collar [3], it is very natural to have such division because the frequency smaller or larger than this thickness shear vibration frequency will mathematically yield two different solution forms. Stephen [9] argued for the physical nonexistence of the second frequency spectrum. While, the experiments [4,8] and computations [5–7,11] show the existence of the second frequency spectrum. For those authors who acknowledges the existence of the second frequency spectrum, the debate still remains [7,8]. By deriving the analytical solutions to the hinged-hinged nonlocal Timoshenko beam, this study presents a different view on the frequency spectrum debate.

On the other hand, the nonlocal elasticity theory [12] is developed by assuming that stress at a point depends not only on the strain at that point but also on strains at all other points of the body. In atomistic simulations, the above assumption can be translated as follows: the forces acting on an atom of a solid are due not only to the nearest neighbor atoms but also to all atoms in the solid [13]. This is another way of stating the long-ranged nature of interatomic forces. In the nonlocal elasticity theory, there is an intrinsic length or lengths measuring the long-ranged effect of interatomic forces [12], which is mainly determined by the inhomogeneity of material microstructure [14]. In comparison, the classical elasticity theory is established by two essential assumptions: homogeneity and ignoring the long-ranged effect of interatomic forces [15], which is thus often referred to as the local theory. Because the nonlocal effect is size-dependent [13,16], which stands out as the structure dimensions diminish, the nonlocal elasticity theory better describes the deformation/motion of a micro/nanometer-scaled structure. For example, the local theory predicts a wrongful dispersion relation, which says that the wave velocity in an elastic continuum increases monotonically and unboundedly as the wave number increases; while, by properly choosing the intrinsic length of the nonlocal effect, the nonlocal theory can match the correct dispersion relation as predicted by lattice dynamics [12]. The nonlocal elasticity has been applied to study the vibration [17–19] and buckling [20,21] of micro/nano-Timoshenko beams, and the vibration of a micro/nano-Euler–Bernoulli beam [22,23]. However, in references [17–19], only the first frequency spectrum is considered. Furthermore, in all of the above studies [17–23], the nonlocal parameter is given *a prior* to examine the nonlocal effect on the micro/nano beam behaviors. In reality, the parameter is an unknown.

* Corresponding author at: State Key Laboratory of Nonlinear Mechanics (LNM), Institute of Mechanics, Chinese Academy of Sciences, Beijing 100190, China.
E-mail address: zhangyin@lnm.imech.ac.cn

http://dx.doi.org/10.1016/j.ijmecsci.2017.05.017
0020-7403/

A comprehensive study is presented by incorporating the nonlocal effect and considering two frequency spectra of a Timoshenko beam. A critical length, which is solely determined by the micro/nano Timoshenko beam cross-section geometry, is identified. If the intrinsic length of nonlocal effect is larger than this critical length, there is only one frequency spectrum in a nonlocal Timoshenko beam; otherwise, there are two frequency spectra like a local Timoshenko beam. Besides the two frequency spectra, a special case called thickness shear vibration, which vibrates at a particular frequency, is also studied. The frequency of thickness shear vibration is shown to be independent on the nonlocal effect. However, whether the thickness shear vibration can occur or not depends on the nonlocal effect. There are three critical frequencies determining the nonlocal Timoshenko beam vibration. One is the frequency of thickness shear vibration, the second one is associated with the intrinsic length of nonlocal effect and shear wave velocity, and the third one is associated with the intrinsic length of nonlocal effect and longitudinal wave velocity. The second and the third frequencies are the asymptotic ones, which physically are also cut-off frequencies. Three nonlocal Timoshenko beams with the hinged–hinged, clamped–clamped and cantilevered boundary conditions are studied. Irrespective of their boundary conditions and insensitive to the beam geometry, the eigenfrequencies of the higher modes of these three beams are all shown to asymptotically approach one of the cut-off frequencies. This asymptotic property can be used as a reliable mechanism to determine the nonlocal effect.

2. Model development

2.1. Governing equations

The free vibration of a nonlocal Timoshenko beam is governed by the following equation

$$\begin{cases} EI\dfrac{\partial^2\phi}{\partial x^2} - \kappa GA\left(\phi + \dfrac{\partial w}{\partial x}\right) = \rho I\left(\dfrac{\partial^2\phi}{\partial t^2} - l^2\dfrac{\partial^4\phi}{\partial x^2\partial t^2}\right) - (1-\alpha)l^2\rho A\dfrac{\partial^3 w}{\partial x\partial t^2}, \\ \kappa GA\left(\dfrac{\partial\phi}{\partial x} + \dfrac{\partial^2 w}{\partial x^2}\right) + \alpha l^2\rho A\dfrac{\partial^4 w}{\partial x^2\partial t^2} = \rho A\dfrac{\partial^2 w}{\partial t^2}, \end{cases} \tag{1}$$

where ϕ and w are the rotation of cross-section and transverse displacement; E and G are the beam Young's modulus and shear modulus; I and A are the second moment of area and cross-section area; ρ and κ are the density and shear correction factor, respectively. Here l is an intrinsic length of nonlocal effect; α is a dimensionless scalar indicator, which takes the value of either 0 or 1. $\alpha = 0$ means that the nonlocal effect is neglected in the shear stress–strain constitutive relation; while, $\alpha = 1$ means that the nonlocal effect is considered in the shear stress–strain constitutive relation [21]. When $\alpha = 1$, Eq. (1) recovers those derived by Li and Wang [17]; when $\alpha = 0$, Eq. (1) recovers those derived by Wang et al. [19]. The detailed derivation of Eq. (1) is given in Appendix A.

The following dimensionless quantities are introduced

$$\xi = \frac{x}{L}, \quad W = \frac{w}{L}, \quad \tau = \sqrt{\frac{EI}{\rho AL^4}}t, \tag{2}$$

where L is the beam length. Eq. (1) is then nondimensionalized as follows

$$\begin{cases} \dfrac{\partial^2\phi}{\partial\xi^2} - R_1\left(\phi + \dfrac{\partial W}{\partial\xi}\right) = R_2\left(\dfrac{\partial^2\phi}{\partial\tau^2} - R_3\dfrac{\partial^4\phi}{\partial\xi^2\partial\tau^2}\right) - (1-\alpha)R_3\dfrac{\partial^3 W}{\partial\xi\partial\tau^2}, \\ R_1\left(\dfrac{\partial\phi}{\partial\xi} + \dfrac{\partial^2 W}{\partial\xi^2}\right) + \alpha R_3\dfrac{\partial^4 W}{\partial\xi^2\partial\tau^2} = \dfrac{\partial^2 W}{\partial\tau^2}. \end{cases} \tag{3}$$

The dimensionless quantities of R_1, R_2 and R_3 are defined as the following

$$R_1 = \frac{\kappa GAL^2}{EI}, \quad R_2 = \frac{I}{AL^2}, \quad R_3 = \frac{l^2}{L^2}. \tag{4}$$

Physically, R_1 indicates the deformation by shear as compared with that by bending; R_2 indicates the geometric slenderness; and R_3 is the squared ratio of the nonlocal effect length to the beam length.

The dimensionless quantities of ϕ and W are assumed to have the following forms

$$\phi(\xi,\tau) = \Phi(\xi)e^{i\omega\tau}, \quad W(\xi,\tau) = Y(\xi)e^{i\omega\tau}. \tag{5}$$

Here ω is the dimensionless circular frequency of vibration. Substituting Eq. (5) into Eq. (3), we have

$$\begin{cases} \dfrac{\partial^2\Phi}{\partial\xi^2} - R_1\left(\Phi + \dfrac{\partial Y}{\partial\xi}\right) = R_2\left(-\omega^2\Phi + R_3\omega^2\dfrac{\partial^2\Phi}{\partial\xi^2}\right) + (1-\alpha)R_3\omega^2\dfrac{\partial Y}{\partial\xi}, \\ R_1\left(\dfrac{\partial\Phi}{\partial\xi} + \dfrac{\partial^2 Y}{\partial\xi^2}\right) - \alpha R_3\omega^2\dfrac{\partial^2 Y}{\partial\xi^2} = -\omega^2 Y \end{cases} \tag{6}$$

The equation set of Eq. (6) consists of two coupled second order ordinary differential equations (ODEs), which can be decoupled. By eliminating Φ, the following uncoupled fourth order ODE for Y is obtained

$$a\frac{\partial^4 Y}{\partial\xi^4} + b\frac{\partial^2 Y}{\partial\xi^2} + cY = 0, \tag{7}$$

where a, b and c are given as follows

$$\begin{aligned} a &= (1 - R_2R_3\omega^2)(R_1 - \alpha R_3\omega^2), \\ b &= (1 - R_2R_3\omega^2)\omega^2 + (R_1 - \alpha R_3\omega^2)(R_2\omega^2 - R_1) \\ &\quad + R_1[R_1 + (1-\alpha)R_3\omega^2], \\ c &= (R_2\omega^2 - R_1)\omega^2. \end{aligned} \tag{8}$$

Similarly, if Y is eliminated, the following uncoupled fourth order ODE for Φ, which is exactly the same form as Eq. (7), is obtained:

$$a\frac{\partial^4\Phi}{\partial\xi^4} + b\frac{\partial^2\Phi}{\partial\xi^2} + c\Phi = 0. \tag{9}$$

2.2. Solution forms

The characteristic equation for both Eqs. (7) and (9) is

$$a\lambda^4 + b\lambda^2 + c = 0, \tag{10}$$

which leads to the following solutions

$$\lambda_1^2 = \frac{-b + \sqrt{b^2 - 4ac}}{2a}, \quad \lambda_2^2 = \frac{-b - \sqrt{b^2 - 4ac}}{2a}. \tag{11}$$

As proved in Appendix B, in all the possible vibration frequency (ω) range of a nonlocal Timoshenko beam, $a = a(\omega)$ and $b = b(\omega)$ as defined in Eq. (8) are always positive. Therefore, λ_2^2 is always negative; λ_1^2 can be either positive or negative depending on the value of ac (or c). In Fig. 1, $ac = (1 - R_2R_3\omega^2)(R_1 - \alpha R_3\omega^2)(R_2\omega^2 - R_1)\omega^2$ is plotted as a function of ω. The expression of ac gives the following three critical frequencies

$$\omega_E = \sqrt{\frac{1}{R_2R_3}}, \quad \omega_S = \sqrt{\frac{R_1}{\alpha R_3}}, \quad \omega_o = \sqrt{\frac{R_1}{R_2}}. \tag{12}$$

To illustrate the physical meanings of these three frequencies, we present them in their dimensional forms. In conjunction with Eqs. (2) and (4), the three dimensional frequencies are given as follows

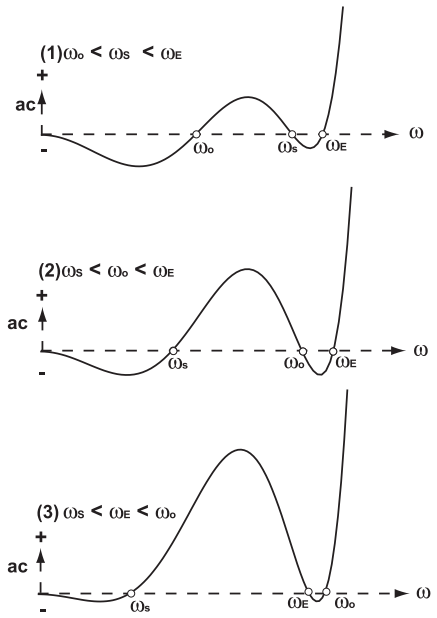

Fig. 1. The schematic sketches on the three scenarios of $ac = (1 - R_2R_3\omega^2)(R_1 - R_3\omega^2)(R_2\omega^2 - R_1)\omega^2$ as a function of ω. (1) $\omega_o < \omega_S < \omega_E$, which corresponds to $R_3 < R_2$ or $l < h/(2\sqrt{3})$. (2) $\omega_S < \omega_o < \omega_E$, which corresponds to $R_2 < R_3 < 1/R_1$ or $h/(2\sqrt{3}) < l < \sqrt{(1+\nu)/(6\kappa)}\,h$. (3) $\omega_S < \omega_E < \omega_o$, which corresponds to $R_3 > 1/R_1$ or $l > \sqrt{(1+\nu)/(6\kappa)}\,h$. Here the three frequencies are defined as $\omega_o = \sqrt{R_1/R_2}, \omega_S = \sqrt{R_1/R_3}$ and $\omega_E = \sqrt{1/(R_2R_3)}$, respectively.

$$\Omega_E = \omega_E\sqrt{\frac{EI}{\rho AL^4}} = \frac{1}{l}\sqrt{\frac{E}{\rho}}, \qquad \Omega_S = \omega_S\sqrt{\frac{EI}{\rho AL^4}} = \frac{1}{l}\sqrt{\frac{\kappa G}{\alpha\rho}},$$
$$\Omega_o = \omega_o\sqrt{\frac{EI}{\rho AL^4}} = \sqrt{\frac{\kappa GA}{\rho I}}. \tag{13}$$

When $\alpha = 0$, Ω_S is infinite, which, as discussed and shown later, is unphysical. From now on, only $\alpha = 1$ is used in our discussion and computation. Here $\sqrt{E/\rho}$ and $\sqrt{G/\rho}$ are the longitudinal and shear wave speeds, respectively. Lei et al. [11] showed that Ω_E and Ω_S are two cut-off frequencies, which means that the vibration frequency of a nonlocal Timoshenko beam cannot surpass either of these two frequencies. Mathematically, these two frequencies are obtained as the asymptotic ones by letting the wave number approach infinity [11]. Another way of viewing these cut-off frequencies in a nonlocal Timoshenko beam is by the wave propagation method, which shows that the wave propagation velocity at a certain large wave number (or frequency) will begin to decrease dramatically and then approach zero [24,25]. Wang and Hu [25] concluded that the microstructure (determining the nonlocal effect) blocks the propagation of waves at a certain high frequency. Ω_o is the frequency of the so-called thickness shear vibration [4,8,10]. Some characteristics of these three critical frequencies can be summarized from Eq. (13) as follows: (1) They are all independent of the boundary conditions and beam length (L); (2) Ω_E depends only on the nonlocal effect (l) and beam material properties (E, ρ), and thus independent of the beam geometry; (3) Ω_S and Ω_o are dependent on the beam cross-section geometry. While, as the shear correction factor, κ, varies only very mildly with different cross-section geometries [26], the Ω_S dependence on the beam geometry is rather weak and is mainly determined by the nonlocal effect and beam material properties; (4) nonlocal effect has no impact on Ω_o.

Here the shear correction factor is taken as $\kappa = 5(1+\nu)/(6+5\nu)$ (ν: Poisson's ratio) because this value is suggested to be the best [9]. With $G = E/2(1+\nu)$ and $\kappa = 5(1+\nu)/(6+5\nu)$, $\Omega_S/\Omega_E = \sqrt{R_1R_2} = \sqrt{\kappa G/E} = \sqrt{5/(12+10\nu)}$ is derived. Therefore, $\Omega_S < \Omega_E$ (or $\omega_S < \omega_E$) always holds in the range of $(0 \le \nu \le 1/2)$. Because $\omega_S < \omega_E$, there are only three possible sequence cases for these three frequencies

(1) $\omega_o < \omega_S < \omega_E$, which corresponds to $R_3 < R_2$.
(2) $\omega_S < \omega_o < \omega_E$, which corresponds to $R_2 < R_3 < 1/R_1$.
(3) $\omega_S < \omega_E < \omega_o$, which corresponds to $R_3 > 1/R_1$.

Because ω_S is the cut-off frequency [11], in cases 2 and 3, $\omega < \omega_S$ always holds and as seen in Fig. 1, $ac < 0$ when $\omega < \omega_S$. Therefore, for cases 2 and 3, λ_1^2 can only be positive. However, in case 1, when $\omega < \omega_o$, $ac < 0$ and λ_1^2 is thus positive; when $\omega_o < \omega < \omega_S$, $ac > 0$ and λ_1^2 is thus negative. Clearly, ω_o is a critical frequency, which determines the solution forms of Eq. (7). $\omega < \omega_o$ and $\omega > \omega_o$ give two different solution forms, which is also the reason why Traill-Nash and Collar said that there are two frequency spectra in the Timoshenko beam vibration [3]. As a convention, $\omega < \omega_o$ is referred to as the first spectrum and $\omega > \omega_o$ as the second spectrum [3]. For case 1 to occur, $R_3 < R_2$ is required, which is equivalent to $l < \sqrt{I/A}$ and $\sqrt{I/A} = h/(2\sqrt{3})$ for a rectangular beam (h: thickness). Therefore, for the vibration of a nonlocal Timoshenko beam, only when $l < \sqrt{I/A}$, can the scenario of two frequency spectra occur.

We should briefly discuss the physical meaning of this critical length $\sqrt{I/A}$. The flexural wave phase velocity of a nonlocal Euler–Bernoulli beam is given as follows [24]

$$V_{ne} = \frac{k}{\sqrt{1+k^2l^2}}\sqrt{\frac{EI}{\rho A}}, \tag{14}$$

where k is the wave number. The following asymptotic phase velocity is obtain as k approaches infinity

$$V_a = \lim_{k\to\infty} V_{ne} = \frac{1}{l}\sqrt{\frac{EI}{\rho A}}. \tag{15}$$

Here the asymptotic phase velocity of V_a is also the maximum velocity. Clearly, $\sqrt{I/A} = V_a/\Omega_E$, which is the quotient of two asymptotic values. This length $\sqrt{I/A}$ can thus be interpreted as the longest traveling distance in the period of $1/\Omega_E$ for the flexural wave of a nonlocal Euler–Bernoulli beam. Physically, the Euler–Bernoulli beam can be viewed as the limit case of the Timoshenko beam as both the rotatory inertia and shear effects approach zero. It is noteworthy to point out that this length $\sqrt{I/A}$, which is solely determined by the beam cross-section geometry, is a measure of the flexural wave traveling distance in a period along the length direction.

There are three solution forms for Eq. (7) depending on the value of ac, i.e., $ac < 0$, $ac > 0$ and $ac = 0$.

1. $ac < 0$

$\lambda_1^2 > 0$ and $\lambda_2^2 < 0$ lead to the following solution forms for Y and Φ.

$$\begin{cases} Y(\xi) = C_1\cosh(\beta_1\xi) + C_2\sinh(\beta_1\xi) + C_3\cos(\beta_2\xi) \\ \qquad + C_4\sin(\beta_2\xi), \\ \Phi(\xi) = D_1\sinh(\beta_1\xi) + D_2\cosh(\beta_1\xi) + D_3\sin(\beta_2\xi) \\ \qquad + D_4\cos(\beta_2\xi). \end{cases} \tag{16}$$

Here β_1 and β_2 are defined as follows

$$\beta_1 = \sqrt{\lambda_1^2} = \sqrt{\frac{-b+\sqrt{b^2-4ac}}{2a}}, \beta_2 = \sqrt{-\lambda_2^2} = \sqrt{\frac{b+\sqrt{b^2-4ac}}{2a}}. \tag{17}$$

C_is and D_is (i=1 to 4) are the unknown constants to be determined by the boundary conditions. C_is and D_is are related by the second equation of Eq. (6), which yields the following:

$$D_1 = \Psi_1C_1, \quad D_2 = \Psi_1C_2, \quad D_3 = \Psi_2C_3, \quad D_4 = -\Psi_2C_4, \tag{18}$$

where Ψ_1 and Ψ_2 are given as follows

$$\Psi_1 = -\frac{(R_1 - R_3\omega^2)\beta_1^2 + \omega^2}{R_1\beta_1}, \quad \Psi_2 = \frac{(R_1 - R_3\omega^2)\beta_2^2 - \omega^2}{R_1\beta_2} \tag{19}$$

Therefore, there are only four rather than eight unknown constants to be determined.

2. $ac > 0$

$\lambda_1^2 < 0$ and $\lambda_2^2 < 0$ lead to the following solution forms for Y and Φ.

$$\begin{cases} Y(\xi) = C_1\cos(\beta_1^*\xi) + C_2\sin(\beta_1^*\xi) + C_3\cos(\beta_2^*\xi) + C_4\sin(\beta_2^*\xi), \\ \Phi(\xi) = D_1\sin(\beta_1^*\xi) + D_2\cos(\beta_1^*\xi) + D_3\sin(\beta_2^*\xi) + D_4\cos(\beta_2^*\xi). \end{cases} \tag{20}$$

Here β_1^* and β_2^* are defined as follows

$$\beta_1^* = \sqrt{-\lambda_1^2} = \sqrt{\frac{b - \sqrt{b^2 - 4ac}}{2a}}, \beta_2^* = \sqrt{-\lambda_2^2} = \sqrt{\frac{b + \sqrt{b^2 - 4ac}}{2a}}. \tag{21}$$

C_is and D_is are now related as the following:

$$D_1 = \Psi_1^* C_1, \quad D_2 = -\Psi_1^* C_2, \quad D_3 = \Psi_2^* C_3, \quad D_4 = -\Psi_2^* C_4, \tag{22}$$

where

$$\Psi_1^* = \frac{(R_1 - R_3\omega^2)\beta_1^{*2} - \omega^2}{R_1\beta_1^*}, \quad \Psi_2^* = \frac{(R_1 - R_3\omega^2)\beta_2^{*2} - \omega^2}{R_1\beta_2^*}. \tag{23}$$

The solution form difference between Eqs. (16) and (20) is noticed. There are two trigonometric functions and two hyperbolic functions in Eq. (16) and four trigonometric functions in Eq. (20). The two trigonometric functions in Eq. (16) stand for the propagating flexural wave [22,27]; the two hyperbolic functions are the non-propagating evanescent components [22]. The four trigonometric functions in Eq. (20) stand for the both the flexural and shear waves [27]. Therefore, the physical difference between the first frequency spectrum and the second frequency spectrum is whether a propagating shear wave coexists with a flexural wave.

3. $ac = 0$

Because $\omega < \omega_S$ and $\omega < \omega_E$, $ac = 0$ is equivalent to $\omega = \omega_o$, which is the scenario of so-called thickness shear vibration. In thickness shear vibration, there is no transverse displacement, i.e., $Y \equiv 0$ [4], and Eq. (9) is reduced to the following (with $\alpha = 1$)

$$\left(1 - R_2R_3\omega_o^2\right)\left(R_1 - R_3\omega_o^2\right)\frac{\partial^4\Phi}{\partial\xi^4} + \left[(1 - R_2R_3\omega_o^2)\omega_o^2 + R_1^2\right]\frac{\partial^2\Phi}{\partial\xi^2} = 0. \tag{24}$$

The solution form of Eq. (24) is as follows:

$$\Phi(\xi) = D_1 + D_2\xi + D_3\cos(\beta_o\xi) + D_4\sin(\beta_o\xi), \tag{25}$$

with β_o defined as follows

$$\beta_o = \sqrt{\frac{(1 - R_2R_3\omega_o^2)\omega_o^2 + R_1^2}{(1 - R_2R_3\omega_o^2)(R_1 - R_3\omega_o^2)}}. \tag{26}$$

The second equation of Eq. (6) still holds, i.e., $R_1\left(\partial\Phi/\partial\xi + \partial^2 Y/\partial\xi^2\right) - R_3\omega^2\partial^2 Y/\partial\xi^2 = -\omega^2 Y$. With $Y \equiv 0$ and $\partial^2 Y/\partial\xi^2 \equiv 0$, we conclude that $\partial\Phi/\partial\xi = D_2 - D_3\beta_o\cos(\beta_o\xi) + D_4\beta_o\cos(\beta_o\xi) = 0$, which leads to $D_2 = D_3 = D_4 = 0$ for arbitrary ξ. Therefore, $\Phi(\xi) = D_1$ and the same result is also obtained by using a wave propagation method [8].

The thickness shear vibration, which only vibrates at $\omega = \omega_o$, is a special scenario of the Timoshenko beam vibration. Abbas and Thomas [5], Bhashymam and Prathap [6] presented an interesting way of viewing the Timoshenko beam vibration, which is the coupling among the vibrations of the Euler–Bernoulli beam, simple shear and pure shear. The thickness shear vibration is shown to be the fundamental mode of the pure shear vibration [6]. For a rectangular beam with $A = bh$ and $I = bh^3/12$ (b, h: beam width and thickness, respectively), the dimensional frequency of Ω_o as given in Eq. (13) is $\Omega_o = \sqrt{\kappa GA/(\rho I)} = \sqrt{12\kappa/(\rho h^2)}$, which is to say that geometrically, this frequency depends on the beam thickness only. Physically, this vibration only occurs in the cross-section and is the type of the pure shear vibration [6]. For these geometric and physical reasons, it is called the thickness shear vibration [8,10]. Because $Y \equiv 0$ and only cross-section rotation, ϕ ($\phi = \Phi e^{i\omega\tau}$ of Eq. (5)), vibrates transversely (in the $y - z$ plane), Downs called this vibration "transverse vibration without transverse deflection" [4]. Because the beam vibration frequency (ω) cannot surpass ω_S, for cases 2 and 3 of $\omega_S < \omega_o < \omega_E$ and $\omega_S < \omega_E < \omega_o$, the thickness shear vibration can not occur. Clearly, whereas the nonlocal effect has no impact on Ω_o (ω_o), Ω_S (ω_S) is determined by the nonlocal effect. Only in the case 1 of $\omega_o < \omega_S < \omega_E$, can the shear thickness vibration occur, which is the same condition for the occurrence of two frequency spectra. Therefore, $l < \sqrt{I/A}$ is the requisite for the occurrence of both two frequency spectra and thickness shear vibration.

2.3. Boundary conditions

In conjunction with Eq. (5), the bending moment M and shear force Q as defined in Eq. (A.8) are now nondimensionalized as follows

$$\bar{M} = \frac{ML}{EI} = e^{i\omega\tau}M_o, \quad \bar{Q} = \frac{QL^2}{EI} = e^{i\omega\tau}Q_o, \tag{27}$$

where M_o and Q_o are given as follows

$$M_o = (1 - R_2R_3\omega^2)\frac{\partial\Phi}{\partial\xi} - R_3\omega^2 Y, \quad Q_o = (R_1 - R_3\omega^2)\frac{\partial Y}{\partial\xi} + R_1\Phi. \tag{28}$$

For the hinged condition, the transverse displacement and moment at the ends are zero, i.e., $Y(\xi_e) = M_o(\xi_e) = 0$ ($\xi_e = 0$ or 1). For the clamped condition, the transverse displacement and cross-section rotation at the ends are zero, i.e., $Y(\xi_e) = \Phi(\xi_e) = 0$ ($\xi_e = 0$ or 1). For the free condition, the moment and shear force at the ends are zero, i.e., $M_o(\xi_e) = Q_o(\xi_e) = 0$ ($\xi_e = 0$ or 1).

3. Results and discussion

The eigenfrequencies of the nonlocal Timoshenko beam with three types of boundary conditions: hinged–hinged, clamped–clamped and cantilever, are examined. The approximate methods may lead to the incomplete solution set of nonlocal beam eigenfrequency [28], the eigenfrequency problem here is formulated to extract its exact values. For all the computations, h/L and ν are fixed as $h/L = 1/5$, $\nu = 0.3$ and $\kappa = 5(1 + \nu)/(6 + 5\nu)$. As a result, the following parameters are also fixed: $R_1 = 100$, $R_2 = 1/300$, $\omega_o = \sqrt{R_1/R_2} = 173.205$ and $E/G = 2(1 + \nu) = 2.6$. R_3 is thus the only varying parameter.

3.1. Hinged–hinged beam

The four boundary conditions are the following

$$Y(0) = 0, \quad M_o(0) = 0, \quad Y(1) = 0, \quad M_o(1) = 0. \tag{29}$$

In conjunction with Eq. (28) and $Y(0) = 0, M_o(0) = 0$ is shown to be equivalent to $\partial\Phi/\partial\xi(0) = 0$. Similarly, in conjunction with Eq. (28) and $Y(1) = 0, M_o(1) = 0$ is shown to be equivalent to $\partial\Phi/\partial\xi(1) = 0$. The hinged–hinged boundary conditions of Eq. (29) can now be written in a more convenient form as follows

$$Y(0) = 0, \quad \frac{\partial\Phi}{\partial\xi}(0) = 0, \quad Y(1) = 0, \quad \frac{\partial\Phi}{\partial\xi}(1) = 0. \tag{30}$$

As discussed in Section 2.2, there are three different solution forms depending on the value of ac. Since $ac = 0$ corresponds to a special scenario of thickness shear vibration whose eigenfrequency is ω_o and its mode shape is easily obtained as presented above, here we only deal with the two cases of $ac < 0$ and $ac > 0$.

For $ac < 0$ and in conjunction with Eqs. (16) and (18), the first two boundary conditions of Eq. (30) are given as follows

$$\begin{cases} C_1 + C_3 = 0, \\ \Psi_1\beta_1 C_1 + \Psi_2\beta_2 C_3 = 0. \end{cases} \tag{31}$$

For Eq. (31) to hold, there are two choices: $\Psi_2\beta_2 - \Psi_1\beta_1 = 0$ or $C_1 = C_3 = 0$. In conjunction with the definitions of Ψ_1 and Ψ_2 in Eq. (19), $\Psi_2\beta_2 - \Psi_1\beta_1 = 0$ can only be satisfied by $\omega = \sqrt{R_1/R_3} = \omega_S$, which is physically impossible. As discussed above, ω_S is a cut-off frequency and all frequencies of a vibrating nonlocal Timoshenko beam must be smaller than this frequency, i.e., $\omega < \omega_S$, which also means $\Psi_2\beta_2 - \Psi_1\beta_1 \neq 0$. Therefore, we have to conclude that $C_1 = C_3 = 0$. With $C_1 = C_3 = 0$, the third and fourth boundary conditions yield the following transcendental equation: $\sinh\beta_1 \sin\beta_2(\Psi_2\beta_2 - \Psi_1\beta_1) = 0$. Because $\Psi_2\beta_2 - \Psi_1\beta_1 \neq 0$, we have $\sinh\beta_1 = 0$ or $\sin\beta_2 = 0$. $\sinh\beta_1 = 0$ leads to $\beta_1 = 0$; with β_1 defined in Eq. (17), $\beta_1 = 0$ yields $ac = 0$, which contradicts with our precondition of $ac < 0$. Therefore, we conclude that $\sinh\beta_1 \neq 0$. Now the only choice is $\sin\beta_2 = 0$, which yields $\beta_2 = n\pi$ (n is a positive integer). With the β_2 definition in Eq. (17), $\beta_2 = n\pi$ gives $(b + \sqrt{b^2 - 4ac})/(2a) = n\pi$ and by performing two successive squaring operations and substitutions of a, b and c as given in Eq. (8), the following equation is obtained

$$a^*\omega^4 + b^*\omega^2 + c^* = 0, \tag{32}$$

where a^*, b^* and c^* are defined as

$$\begin{aligned} a^* &= R_2(n^4\pi^4R_3^2 + 2n^2\pi^2R_3 + 1), \\ b^* &= -[n^4\pi^4R_3(1 + R_1R_2) + n^2\pi^2(1 + R_1R_2 + R_1R_3) + R_1], \\ c^* &= n^4\pi^4R_1. \end{aligned} \tag{33}$$

The two roots of Eq. (32) are obtained as follows

$$\omega_{1,2}^2 = \frac{-b^* \pm \sqrt{b^{*2} - 4a^*c^*}}{2a^*}. \tag{34}$$

Both ω_1^2 and ω_2^2 yield positive values; because $\omega_1^2 > \omega_2^2, \omega_1^2$ is referred to as the upper root and ω_2^2 as lower root [3]. When R_2 becomes vanishingly small, the upper root tends to infinity, which is unphysical and thus must be discarded. In Eq. (34), only the lower root should be kept, i.e.,

$$\omega^2 = \frac{-b^* - \sqrt{b^{*2} - 4a^*c^*}}{2a^*} \tag{35}$$

For a local Timoshenko beam, i.e., $R_3 = 0$, Eq. (35) gives the following result

$$\omega^2 = \frac{n^2\pi^2(1 + R_1R_2) + R_1 - \sqrt{[n^2\pi^2(1 + R_1R_2) + R_1]^2 - 4n^4\pi^4R_1R_2}}{2R_2}. \tag{36}$$

The shear effect on the Timoshenko beam eigenfrequencies is much larger than that of the rotatory inertia [3]. For a local Timoshenko beam with no rotatory inertia effect, i.e., $R_2 = R_3 = 0$, Eq. (32) becomes the following

$$-(n^2\pi^2 + R_1)\omega^2 + n^4\pi^4R_1 = 0, \tag{37}$$

which yields

$$\omega^2 = \frac{n^4\pi^4R_1}{n^2\pi^2 + R_1}. \tag{38}$$

It is noted that the limit of Eq. (38) yields $\lim_{R_1\to\infty}\omega^2 = n^4\pi^4R_1/(n^2\pi^2 + R_1) = n^4\pi^4$, which recovers the eigenfrequencies of the hinged–hinged local Euler–Bernoulli beam.

For $ac < 0$, following the same derivation procedures presented above, we arrives at the transcendental equation of $\sin\beta_1^*\sin\beta_2^*(\Psi_2\beta_2^* - \Psi_1\beta_1^*) = 0$, which leads to $\beta_1^* = n\pi$ and $\beta_2^* = n\pi$. In conjunction with the definitions of β_1^* and β_2^* in Eq. (21), both $\beta_1^* = n\pi$ and $\beta_2^* = n\pi$ yield the same equation as Eq. (32), which is somewhat surprising and worthy of some comments. Physically, $ac < 0$ means $\omega < \omega_o$ and $ac > 0$ means $\omega > \omega_o$; and mathematically, these two scenarios also generate two different solution forms for Y and Φ. However, the two different solution forms lead to the same eigenfrequency expression of Eq. (35). When the integer n changes, the eigenfrequency (ω) obtained by either Eq. (35) or Eq. (36) or Eq. (38) can be either larger or smaller than ω_o. Because the solution form prescribes one frequency spectrum, the final derivation of eigenfrequency covers both frequency spectra regardless of the solution form. Therefore, there is a logic inconsistency here, which is also noticed by Levinson and Cooke [7] in a different way. They [7] showed that the eigenfrequency larger than ω_o can be obtained by the solution form of the first frequency spectrum for a hinged–hinged (local) Timoshenko beam; and about this logic inconsistency, they concluded that "the shear mode frequency (which is ω_o here) is *not* a boundary between 'two frequency spectra'." However, we must emphasize here that this conclusion only holds for the hinged–hinged Timoshenko beam. For other types of boundary conditions such as clamped–clamped and cantilevered ones as discussed later, the eigenfrequency larger than ω_o can only be obtained by the solution form of the second frequency spectrum and the eigenfrequency smaller than ω_o can only be obtained by the solution form of the first frequency spectrum. That the two different solution forms lead to the same eigenfrequency expression for the hinged–hinged beam, by our opinion, is purely coincidence.

The nth eigenfrequency of ω_n is obtained by Eq. (35). Because it is customary to present the square root of the (dimensionless) eigenfrequency [19,22,29]. the variations of the first twelve γ_ns ($\gamma_n = \sqrt{\omega_n}$) as the functions of R_3 are presented in Table 1. The corresponding γ_ns of the local Euler–Bernoulli (LEB) beam [29] are also presented for comparison reason. In this study, all parameters except R_3 are fixed and $\gamma_o = \sqrt{\omega_o} = (R_1/R_2)^{1/4} = 13.161$. It is observed that as R_3 increases, all γ_ns (eigenfrequencies) monotonically decrease, which is more straightforwardly demonstrated in Figs. 2 and 3. Furthermore, the γ_ns of higher modes decreases much more dramatically than those of lower modes as R_3 increases, which can be clearly seen in Table 1. The nonlocal effect is size-dependent, which is determined by three sizes: the unit cell/microstructure size, the specimen size and the wavelength of variation of the applied mechanical field [30]. At higher modes, the wavelength is shorter and the nonlocal effect is thus more prominent, which, as a result, leads to larger decreases of eigenfrequencies of higher modes [23]. Fig. 2 plots γ_1, γ_2 and γ_3 as the functions of R_3. Fig. 3 plots γ_{10}, γ_{11} and γ_{12} as the functions of R_3. In Fig. 3, $\gamma_o = 13.161$ is plotted as a horizontal line. $\gamma_S = \sqrt{\omega_S} = (R_1/R_3)^{1/4}$ is also plotted. In Table 1 and Fig. 3, it is observed that in certain range of R_3, some γ_ns (eigenfrequencies) are larger than $\gamma_o = 13.161$, which is of the second frequency spectrum. For example, in Table 1, when $R_3 = 10^{-4}$, γ_ns with $n \geq 7$ are larger than γ_o. While, when $R_3 = 10^{-2}$ or larger, none of γ_ns is larger than γ_o. The reason is explained in Fig. 1. For the Timoshenko beam eigenfrequency to be in the second frequency spectrum, i.e., larger than γ_o, R_3 needs to be smaller than R_2. Only when $R_3 < R_2 = 1/300$, can some γ_ns surpass the value of $\gamma_o = 13.161$. Therefore, when $R_3 < R_2 = 1/300$, there are two frequency spectra; when $R_3 > R_2 = 1/300$, there is only the first frequency spectrum. In Fig. 2, γ_1, γ_2 and γ_3 are fairly well-separated and the gap distance among them shrinks with the increase of R_3. In Fig. 3, the gap distance among γ_{10}, γ_{11} and γ_{12} is so small that three γ_ns almost stick together. Furthermore, the gap distance between γ_n and γ_{n+1} decreases as mode number n increases, which can be seen more clearly in Table 1. Lei et al. call this phenomenon as "the clustering of vibration modes in the higher frequency range" [11]. The reason for the gap distance shrinking or the clustering of higher modes is the one mentioned above: the nonlocal effect causes the larger eigenfrequency

Table 1
Variation of the first twelve γ_ns ($\gamma_n = \sqrt{\omega_n}$) of the hinged–hinged nonlocal Timoshenko beam with the nonlocal parameter R_3. $R_3 = 0$ corresponds to the local Timoshenko beam case and the γ_ns of local Euler–Bernoulli (LEB) beam are also given.

R_3	γ_1	γ_2	γ_3	γ_4	γ_5	γ_6	γ_7	γ_8	γ_9	γ_{10}	γ_{11}	γ_{12}
0	3.048	5.686	7.870	9.706	11.289	12.686	13.943	15.091	16.152	17.142	18.073	18.955
10^{-4}	3.047	5.680	7.853	9.668	11.220	12.576	13.779	14.861	15.844	16.743	17.571	18.336
2×10^{-4}	3.046	5.674	7.836	9.631	11.154	12.470	13.625	14.649	15.564	16.387	17.131	17.806
10^{-2}	2.977	5.231	6.714	7.659	8.273	8.685	8.971	9.176	9.327	9.441	9.529	9.598
0.1	2.567	3.812	4.439	4.795	5.015	5.160	5.260	5.332	5.385	5.425	5.456	5.480
LEB	π	2π	3π	4π	5π	6π	7π	8π	9π	10π	11π	12π

decreases of higher modes [23]. In contrast, the gap distance between γ_n and γ_{n+1} of a local Euler–Bernoulli beam is the constant of π. It is also seen that in Fig. 3, all three γ_ns are below the curve of γ_S. Actually, all γ_ns are below the curve of γ_S. Again, the reason is that γ_S is a square root of a cut-off frequency and thus, physically no γ_n can be larger than γ_S [11]. It is noteworthy to mention that γ_S intersects $\gamma_o = 13.161$ at $R_3 = 1/300 = R_2$.

3.2. Clamped–clamped beam

The four boundary conditions are the following

$$Y(0) = 0, \quad \Phi(0) = 0, \quad Y(1) = 0, \quad \Phi(1) = 0. \tag{39}$$

For $ac < 0$, in conjunction with Eq. (18), by substituting Eq. (16) into Eq. (39), the eigenfrequency of a clamped–clamped beam is determined by the following equation

$$\begin{vmatrix} 1 & 0 & 1 & 0 \\ 0 & \Psi_1 & 0 & -\Psi_2 \\ \cosh\beta_1 & \sinh\beta_1 & \cos\beta_2 & \sin\beta_2 \\ \Psi_1\sinh\beta_1 & \Psi_1\cosh\beta_1 & \Psi_2\sin\beta_2 & -\Psi_2\cos\beta_2 \end{vmatrix} = 0, \tag{40}$$

where β_1 and β_2 are given in Eq. (17); Ψ_1 and Ψ_2 are given in Eq. (19).

For $ac > 0$, in conjunction with Eq. (22), by substituting Eq. (20) into Eq. (39), the following equation is obtained

$$\begin{vmatrix} 1 & 0 & 1 & 0 \\ 0 & \Psi_1^* & 0 & \Psi_2^* \\ \cos\beta_1^* & \sin\beta_1^* & \cos\beta_2^* & \sin\beta_2^* \\ \Psi_1^*\sin\beta_1^* & -\Psi_1^*\cos\beta_1^* & \Psi_2\sin\beta_2^* & -\Psi_2\cos\beta_2^* \end{vmatrix} = 0, \tag{41}$$

where β_1^* and β_2^* are given in Eq. (21); Ψ_1^* and Ψ_2^* are given in Eq. (23).

Unlike the analytical derivations for the hinged–hinged beam, the eigenfrequencies of the clamped–clamped beam are determined by the transcendental equations of Eqs. (40) and (41), which have to be solved numerically by the Newton–Raphson method [31]. When applying the Newton–Raphson method to find the eigenfrequencies, we need to switch between Eqs. (40) and (41) depending on whether $\omega < \omega_o$ or $\omega > \omega_o$. The variations of the first twelve γ_ns ($\gamma_n = \sqrt{\omega_n}$) as the functions of R_3 together with those of the local Euler–Bernoulli beam [29] are presented in Table 2. In Fig. 4, γ_1, γ_2 and γ_3 are plotted and in Fig. 5, γ_{10}, γ_{11} and γ_{12} are plotted. Except the differences in values, the γ_ns of the clamped–clamped beam share the following four trends with those of the hinged–hinged beam: (1) All γ_ns decreases monotonically as R_3 increases and the R_3 impact on the γ_ns of higher modes is much more significant; (2) the gap distance between γ_n and γ_{n+1} becomes smaller as the mode number n increases, i.e., "the clustering of vibration modes" [11] occurs; (3) all γ_n curves are under/smaller than the asymptotic γ_S curve; (4) when $R_3 < R_2 = 1/300$, there are two frequency spectra; when $R_3 > R_2$, there is only the first frequency spectrum.

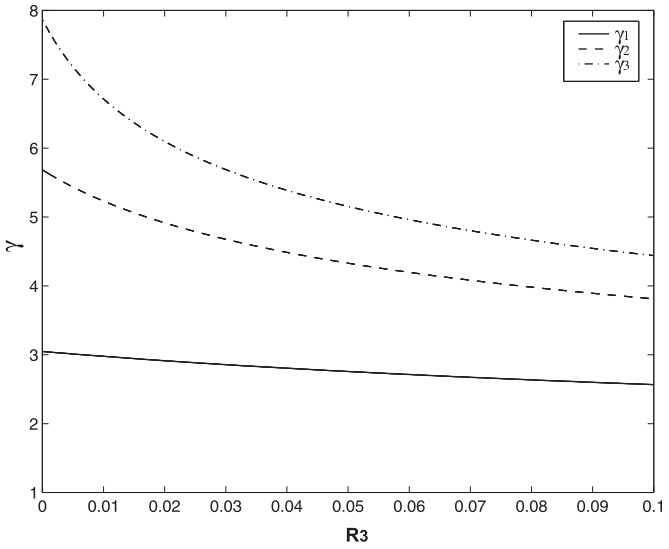

Fig. 2. γ_1, γ_2 and γ_3 of a hinged–hinged beam as the functions of R_3. Here γ_i is the square root of the eigenfrequency, i.e., $\gamma_i = \sqrt{\omega_i}$.

In the computation of the eigenfrequencies of the clamped–clamped beam, there are two distinct facts as compared with that of the hinged–hinged beam. Firstly, the eigenfrequency of the first frequency spectrum is obtained from Eq. (40) and that of the second frequency spectrum is obtained from Eq. (41). Eqs. (40) and

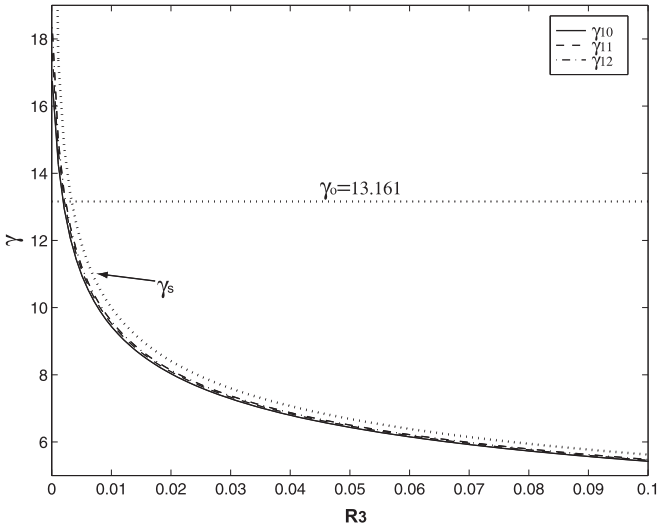

Fig. 3. γ_{10}, γ_{11} and γ_{12} of a hinged–hinged beam as the functions of R_3. The horizontal straight line is $\gamma_o = \sqrt{\omega_o} = 13.161$. ω_o is the frequency of the thickness shear vibration. The square root of the asymptotic shear frequency, i.e., $\gamma_S = \sqrt{\omega_S}$, as a function of R_3 is also plotted.

(41) result from two different solution forms and different solution form prescribes different frequency spectrum. It is a unique and unusual scenario for the hinged–hinged beam that the two different solution forms lead to the same eigenfrequency expression, which covers two frequency spectra. Secondly, in the analytical derivations of the hinged–hinged beam, the usage of ω_S as a cut-off frequency is a crucial one in the whole derivation. In contrast, no (explicit) cut-off frequency information in Eqs. (40) and (41) is used.

3.3. Cantilever beam

The four boundary conditions are the following

$$Y(0) = 0, \quad \Phi(0) = 0, \quad M_o(1) = 0, \quad Q_o(1) = 0. \tag{42}$$

For $ac < 0$, in conjunction with Eqs. (18) and (28), by substituting Eq. (16) into Eq. (42), the eigenfrequency of a cantilever beam is determined by the following equation

$$\begin{vmatrix} 1 & 0 & 1 & 0 \\ 0 & \Psi_1 & 0 & -\Psi_2 \\ f_1\cosh\beta_1 & f_1\sinh\beta_1 & f_2\cos\beta_2 & f_2\sin\beta_2 \\ f_3\sinh\beta_1 & f_3\cosh\beta_1 & f_4\sin\beta_2 & -f_4\cos\beta_2 \end{vmatrix} = 0, \tag{43}$$

where f_is are defined as follows

$$f_1 = (1 - R_2R_3\omega^2)\Psi_1\beta_1 - R_3\omega^2, \quad f_2 = (1 - R_2R_3\omega^2)\Psi_2\beta_2 - R_3\omega^2,$$
$$f_3 = (R_1 - R_3\omega^2)\beta_1 + R_1\Psi_1, \quad f_4 = -(R_1 - R_3\omega^2)\beta_2 + R_1\Psi_2, \tag{44}$$

where β_1 and β_2 are given in Eq. (17); Ψ_1 and Ψ_2 are given in Eq. (19).

For $ac > 0$, in conjunction with Eq. (22) and (28), by substituting Eq. (20) into Eq. (42), the following equation is obtained

$$\begin{vmatrix} 1 & 0 & 1 & 0 \\ 0 & \Psi_1^* & 0 & \Psi_2^* \\ f_1^*\cos\beta_1^* & f_1^*\sin\beta_1^* & f_2^*\cos\beta_2^* & f_2^*\sin\beta_2^* \\ f_3^*\sin\beta_1^* & -f_3^*\cos\beta_1^* & f_4^*\sin\beta_2^* & -f_4^*\cos\beta_2^* \end{vmatrix} = 0, \tag{45}$$

where f_i^*s are defined as follows

$$f_1^* = (1 - R_2R_3\omega^2)\Psi_1^*\beta_1^* - R_3\omega^2, \quad f_2^* = (1 - R_2R_3\omega^2)\Psi_2^*\beta_2^* - R_3\omega^2,$$
$$f_3^* = -(R_1 - R_3\omega^2)\beta_1^* + R_1\Psi_1^*, \quad f_4^* = -(R_1 - R_3\omega^2)\beta_2^* + R_1\Psi_2^*, \tag{46}$$

where β_1^* and β_2^* are given in Eq. (21); Ψ_1^* and Ψ_2^* are given in Eq. (23).

The variations of the γ_ns ($\gamma_n = \sqrt{\omega_n}$) are presented in Table 3, Figs. 6 and 7. The trends are the same as summarized in the above section except a striking difference: γ_1 monotonically increases while all other γ_ns decrease as usual with the increase of R_3. In Table 3, at $R_3 = 0.1, \gamma_1 = 1.883$, which is even larger than $\gamma_1 = 1.875$ as predicted by the local Euler–Bernoulli beam model. The abnormal γ_1 increasing behavior with R_3 is also verified by the finite element analysis. This abnormal phenomenon is also observed by

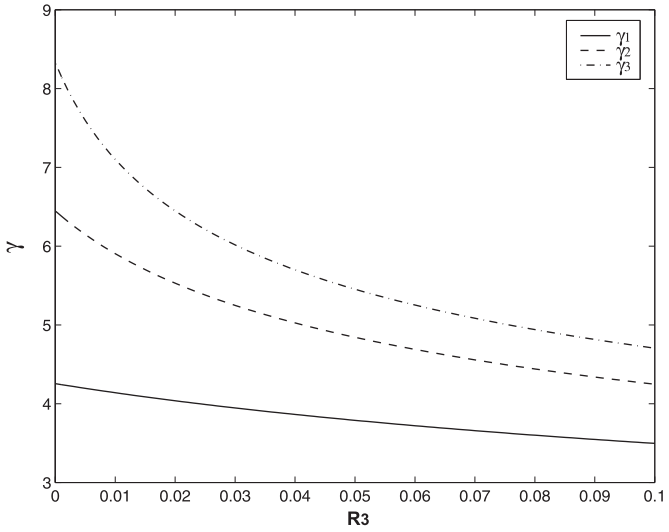

Fig. 4. γ_1, γ_2 and γ_3 of a clamped–clamped beam as the functions of R_3.

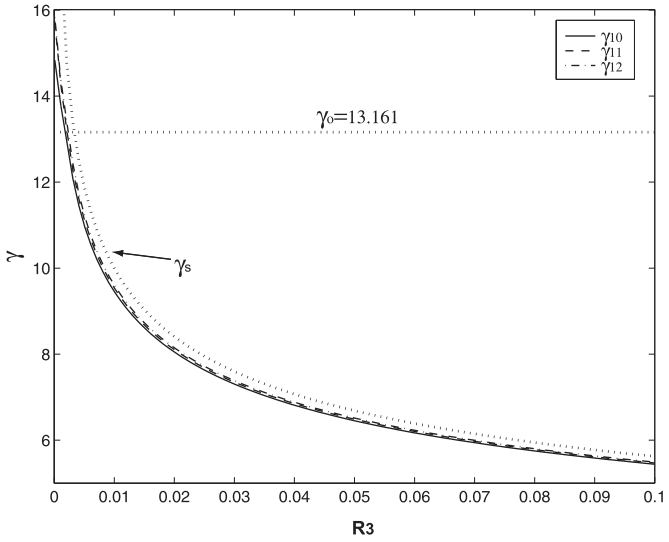

Fig. 5. γ_{10}, γ_{11} and γ_{12} of a clamped–clamped beam as the functions of R_3. The dotted lines are the horizontal $\gamma_o = \sqrt{\omega_o} = 13.161$ and the asymptotic γ_S, respectively.

Wang et al. [19] in a nonlocal cantilever Timoshenko beam and by Lu et al. [22], and Xu [23] in a nonlocal cantilever Euler–Bernoulli beam. Xu even found that the first two eigenfrequencies of a nonlocal cantilever Euler–Bernoulli beam are larger than those of a local one [23]. This abnormal phenomenon is somewhat puzzling. Because the presence of rotatory inertia and shear force, which increases the system inertia and decreases the system stiffness, the γ_ns predicted by the local Timoshenko beam model are always smaller than those by the local Euler–Bernoulli beam model.

Table 2
Variation of the first twelve γ_ns ($\gamma_n = \sqrt{\omega_n}$) of the clamped–clamped nonlocal Timoshenko beam with the nonlocal parameter R_3. $R_3 = 0$ corresponds to the local Timoshenko beam case and the γ_ns of local Euler–Bernoulli (LEB) beam are also given.

R_3	γ_1	γ_2	γ_3	γ_4	γ_5	γ_6	γ_7	γ_8	γ_9	γ_{10}	γ_{11}	γ_{12}
0	4.256	6.449	8.333	9.966	11.424	12.729	13.577	13.910	14.589	15.049	15.797	16.127
10^{-4}	4.254	6.442	8.314	9.927	11.357	12.624	13.569	13.763	14.555	14.840	15.736	15.838
2×10^{-4}	4.253	6.436	8.296	9.890	11.291	12.523	13.561	13.620	14.526	14.641	15.570	15.679
10^{-2}	4.140	5.905	7.102	7.879	8.404	8.765	9.023	9.210	9.351	9.457	9.541	9.607
0.1	3.497	4.248	4.705	4.945	5.119	5.224	5.308	5.363	5.410	5.442	5.470	5.490
LEB	4.730	7.853	10.995	14.137	17.279	20.420	23.562	26.704	29.845	32.987	36.128	39.270

Furthermore, the presence of the nonlocal effect is to decrease the system stiffness and thus eigenfrequencies as observed in both nonlocal hinged–hinged and clamped–clamped Timoshenko beams. Another example on the nonlocal effect reducing system stiffness is in statics: the buckling loads with different boundary conditions including the cantilevered ones all monotonically decrease with the increase of nonlocal effect (R_3); and the nonlocal Timoshenko beam model predicts smaller buckling loads than those by the local Euler–Bernoulli beam model for the beams with all different boundary conditions [20]. The static buckling of a beam can be viewed dynamically as that its first eigenfrequency approaches zero [32]. One explanation for this abnormal phenomenon is that the buckling problem of nonlocal beams (Euler–Bernoulli and Timoshenko) is self-adjoint for all types of boundary conditions; while, the bending vibration problem of the nonlocal cantilever beam is a special one, which is nonself-adjoint [33]. The nonself-adjointness property can be attributed to a non-conservative inertia moment acting on the beam free end [33], which cannot be derived from a potential [33,34]. Reddy and El-Borgi [34] pointed out that it is not possible to construct the underlying quadratic functionals for nonlocal beam theories. According to Fernández-Sáez et al. [35], the nonself-adjointness is also responsible for another problem that in a nonlocal Euler–Bernoulli beam depending on the nonlocal parameter l, only a few or even none of the natural frequencies can be calculated [22]. The nonself-adjointness problem can be corrected by the following two ways: One is to construct a functional by an inverse procedure, which in essence modifies the boundary conditions of the nonlocal cantilever beam as given in Eq. (42) to make the problem self-adjoint [33]. The other is to formulate the nonlocal problem by the integral form [35]. In comparison, Eq. (1) is the differential formulation as reflected by Eq. (A.2).

This abnormal behavior can also be explained from another different angle. Romano et al. [36] argued that due to the differential formulation, the nonlocal beam bending problem must satisfy additional constraint conditions called constitutive boundary conditions to assure the existence and uniqueness of the solution. While, the constitutive boundary conditions are incompatible with the equilibrium equation in the bending field. Therefore, no bending field solution in general exists [36]. If Romano's statics conclusion is extended to dynamics, this abnormal behavior is caused by Eq. (16) because it cannot satisfy the constitutive boundary conditions and it is thus not a real solution.

3.4. Vibration of higher modes as a mechanism to determine the nonlocal effect

Although the first mode of the cantilever beam shows some abnormal behaviors, it is noticed that Figs. 3, 5 and 7 are almost the same: the γ_ns of higher modes all approach γ_S and their differences shrink as R_3 increases. For example, at $R_3 = 10^{-4}$, γ_{12}=18.336, 15.838, 15.406 for the hinged–hinged, clamped–clamped and cantilevered beams, respectively; and at $R_3 = 0.1$, γ_{12}=5.480, 5.490, 5.466 for the hinged–hinged, clamped–clamped and cantilevered beams, respectively. It is noticed that in Tables 1–3, as the mode number changes, the gap distance between γ_n and γ_{n+1} fluctuates mildly around 3 for the local Euler–Bernoulli beams with three different boundary conditions. In contrast, for a nonlocal Timoshenko beam, the gap distance between γ_n and γ_{n+1} shrinks dramatically as either mode number or R_3 increases. This gap distance shrinking phenomenon of eigenfrequency is also observed by Wang et al. for a nonlocal Timoshenko beam [19] and by Lu et al. for a nonlocal Euler–Bernoulli beam [22]. Boundary conditions have very little impact on the eigenfrequency variations of higher modes with R_3. The facts of the γ_ns of higher modes approaching γ_S and their shrinking gap

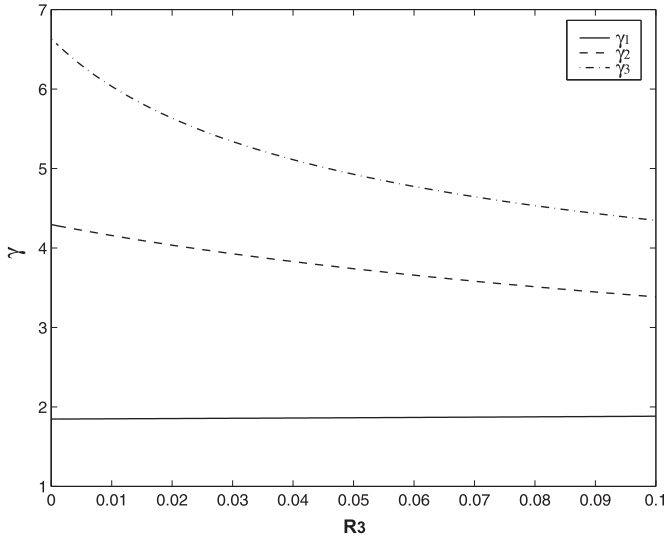

Fig. 6. γ_1, γ_2 and γ_3 of a cantilever beam as the functions of R_3.

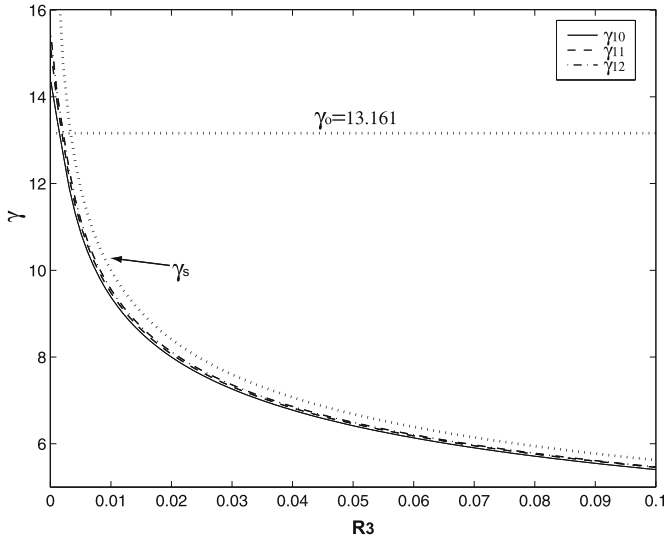

Fig. 7. γ_{10}, γ_{11} and γ_{12} of a cantilever beam as the functions of R_3. The dotted lines are the horizontal $\gamma_o = \sqrt{\omega_o} = 13.161$ and the asymptotic γ_S, respectively.

Table 3
Variation of the first twelve γ_ns ($\gamma_n = \sqrt{\omega_n}$) of the cantilever nonlocal Timoshenko beam with the nonlocal parameter R_3. $R_3 = 0$ corresponds to the local Timoshenko beam case and the γ_ns of local Euler–Bernoulli (LEB) beam are also given.

R_3	γ_1	γ_2	γ_3	γ_4	γ_5	γ_6	γ_7	γ_8	γ_9	γ_{10}	γ_{11}	γ_{12}
0	1.847	4.295	6.635	8.559	10.214	11.644	12.872	13.467	14.059	14.443	15.215	15.582
10^{-4}	1.847	4.293	6.628	8.538	10.172	11.574	12.775	13.431	13.961	14.346	15.086	15.406
2×10^{-4}	1.847	4.292	6.620	8.517	10.131	11.506	12.679	13.389	13.867	14.252	14.953	15.248
10^{-2}	1.851	4.157	6.034	7.211	7.980	8.483	8.830	9.074	9.252	9.384	9.485	9.563
0.1	1.883	3.385	4.349	4.679	4.998	5.106	5.257	5.300	5.385	5.404	5.457	5.466
LEB	1.875	4.694	7.855	10.996	14.137	17.279	20.420	23.562	26.704	29.845	32.987	36.128

distances are responsible for the so-called "the clustering of vibration modes in the higher frequency range" [11].

The intrinsic length of nonlocal effect, l, is often written as $l = e_o a$ [12,19,20,22]. Here a is the elastic body internal length such as lattice parameter or grain size, and e_o is a constant to be determined for each material. The nonlocal effect indicated by l is determined by the inhomogeneity of material microstructure [14]. Generally speaking, the nonlocal effects in amorphous solids are larger than those of crystalline solids [14]. So far, there are still no definite experimental methods of determining l or e_o. An effective way of finding l or e_o is to match the results predicted by the nonlocal theories of elastic continuum with those by the discrete atomistic simulation or lattice dynamics. For example, Eringen [12] found $e_o = 0.39$ by matching the dispersion relation predicted by the nonlocal elasticity theory with that by Born–Kármán model of lattice dynamics. However, it should keep in mind that different matching methods may give quite different results. For example, by matching the buckling strains of carbon nanotubes (CNT) predicted by the nonlocal elasticity theory and by the molecular mechanics simulation, Zhang et al. found $e_o = 0.82$ [37]; while, Sudak found $e_o = 112.7$ [38]. By matching the transverse deflections predicted by the nonlocal elasticity theory and by the molecular dynamics simulation, Liang and Han [39] found that rather than a constant, the e_o for a CNT depends on its chirality and geometry, which is fitted as $e_o = 0.0297R/a + 0.204$ for the zigzag CNT and $e_o = 0.052R/a + 0.1528$ for the armchair CNT (R: CNT radius). Wang et al. [19] showed that e_o may even vary in a large range when a CNT vibrates transversely at different frequencies. Zhang et al. [40] found that the e_o of a nonlocal beam varies (mildly) with different boundary conditions when an axial force is present. Besides the difficulty and inconsistency in the above matching methods, boundary conditions, which are a big issue in the micromechanics tests, also play a key role [19,37,39,40]. In contrast, γ_S (or Ω_S) is independent of the boundary conditions. Furthermore, as defined in Eq. (13), Ω_S is independent of the beam length and insensitive to the beam cross-section geometry (as embodied in κ). Therefore, the asymptotic property of the eigenfrequencies of higher modes can be used as a reliable mechanism to determine the nonlocal effect: once the eigenfrequency of a higher mode is measured, which is (close to) Ω_S, the nonlocal effect l is then easily determined by Eq. (13).

It should be noted that, whereas the number of modes in the continuum Timoshenko beam is infinite, the number of modes in the lattice beam is equal to the number of layers. The differential equation (such as Eq. (1)) of an elastic continuum in essence is the long wave, low frequency limit of the finite difference equation of lattice dynamics [41]. With the increase of mode number, frequency increases and wave length decreases, the lattice mode shape will deviates more and more from the sinusoidal form (as given in Eq. (20)) characteristic of the continuum [41], which leads to an increasing error and final break-down of the continuum theory. Therefore, for a nanometer scaled beam, one should be cautious about the validity of the higher modes' eigenfrequencies computed by the nonlocal continuum theory.

3.5. Comparison of nonlocal Timoshenko and nonlocal Euler–Bernoulli beams

The eigenfrequencies predicted by the nonlocal Timoshenko and nonlocal Euler–Bernoulli beam theories are compared in Fig. 8. In Fig. 8, (a), (b) and (c) are the γ_1s of the hinged-hinged, clamped–clamped and cantilever beams, respectively; (d), (e) and (f) are the γ_2s of the hinged-hinged, clamped–clamped and cantilever beams, respectively. The nonlocal Euler–Bernoulli beam theory and its derivation on the eigenfrequency computation are presented in Appendix C. In all the cases, the eigenfrequencies predicted by the nonlocal Euler–Bernoulli beam theory are always larger than those by the nonlocal Timoshenko beam theory. The reasons are that in the Timoshenko beam model, the rotatory inertia effect (the $\rho I\partial^2\phi/\partial^2 t$ term in Eq. (1)) and shear force effect (the $\kappa GA(\phi + \partial w/\partial x)$ term in Eq. (1)) are considered. The rotatory inertia increases the system effective mass and shear force decreases the system stiffness. As a result, the Timoshenko beam theory leads to lower eigenfrequencies than those by the Euler–Bernoulli beam theory. It is also noticed that in Fig. 8(c), the abnormal behavior of γ_1 increasing with R_3 is also captured by the nonlocal Euler–Bernoulli beam theory. Another characteristics noticed is that the γ_2 differences predicted by the nonlocal Timoshenko and Euler–Bernoulli beam theories are larger than those of γ_1 for all three beams with different boundary conditions.

4. Conclusions

To model a nonlocal Timoshenko beam, the nonlocal shear effect must be considered. Otherwise, it leads to an infinite ω_S, which is unphysical. There are three frequencies (ω_S, ω_E and ω_o) determining the vibration behavior of a nonlocal Timoshenko. Since $\omega_S < \omega_E$ for an isotropic Timoshenko beam, ω_o and ω_S are the two *defacto* frequencies playing the roles: ω_o determines the solution forms; ω_S is the cut-off frequency; when $\omega_o < \omega_S$, there are two frequency spectra and thickness shear vibration; when $\omega_o > \omega_S$, there is only the first frequency spectrum. For a rectangular Timoshenko beam, $\omega_o < \omega_S$ also leads to an important geometric relation of $l < \sqrt{I/A}$ and $\sqrt{I/A} = h/(2\sqrt{3})$ for a rectangular beam (h: thickness). As l measures the nonlocal effect, $h/(2\sqrt{3})$ is a critical length determining the beam frequency spectra: when nonlocal effect is weak, i.e., $l < h/(2\sqrt{3})$, there are two frequency spectra and thickness shear vibration; when nonlocal effect is strong, i.e., $l > h/(2\sqrt{3})$, there is only the first frequency spectrum. Boundary conditions have significant impact on the eigenfrequencies of lower modes and much less impact on those of higher modes. The eigenfrequencies with large mode numbers asymptotically approach ω_S. "The clustering of vibration modes in the higher frequency range" phenomenon [11] is caused by that the nonlocal effect on different vibration mode is different. Because ω_S is independent of the boundary boundary conditions, the beam length and insensitive to the beam cross-section geometry, which is a huge advantage in the micro/nanomechanics test, it is suggested as a new and reliable method to determine the nonlocal effect.

Acknowledgments

This work was supported by the National Natural Science Foundation of China (NSFC No. 11372321).

Appendix A. Derivation of the governing equations for the nonlocal Timoshenko beam vibration

The kinematic assumptions of the Timoshenko beam model are the followings [17]

$$\epsilon_{xx} = z\frac{\partial\phi}{\partial x}, \quad \epsilon_{xz} = \frac{1}{2}\left(\phi + \frac{\partial w}{\partial x}\right), \tag{A.1}$$

where ϵ_{xx} and ϵ_{xz} are the normal axial strain and shear strain; ϕ is the rotation of cross-section and w is the transverse displacement. Here x, y and z are the directions along the beam length, width and thickness, respectively. A generalized nonlocal constitutive relations are given as follows [21]

$$\sigma_{xx} - l^2\frac{\partial^2\sigma_{xx}}{\partial x^2} = E\epsilon_{xx}, \quad \sigma_{xz} - \alpha l^2\frac{\partial^2\sigma_{xz}}{\partial x^2} = 2G\epsilon_{xz}, \tag{A.2}$$

where σ_{xx} and σ_{xz} are the normal and shear stresses, respectively. E is the Young's modulus and G is the shear modulus. l is an intrinsic

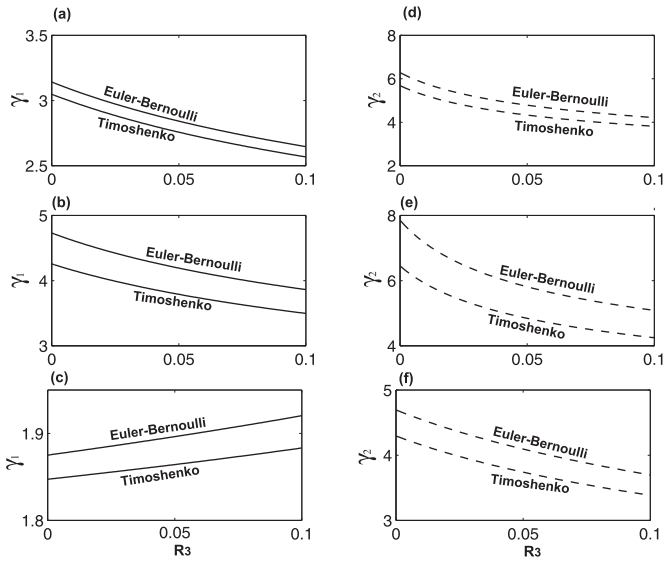

Fig. 8. (a), (b) and (c) are the γ_1s of the nonlocal hinged–hinged, clamped–clamped and cantilever beams, respectively. (d), (e) and (f) are the γ_2s of the nonlocal hinged–hinged, clamped–clamped and cantilever beams, respectively.

length of nonlocal effect and α is a dimensionless scalar indicator.

By definition, the bending moment (M) and shear force (Q) are given as

$$M = \int_A z\sigma_{xx}dA, \quad Q = \int_A \sigma_{xz}dA = 2G\epsilon_{xz}. \tag{A.3}$$

where A is the cross-section area. Substituting the constitutive relations of Eq. (A.2) into Eq. (A.3) leads to the following

$$M - l^2\frac{\partial^2 M}{\partial x^2} = EI\frac{\partial \phi}{\partial x}, \quad Q - \alpha l^2\frac{\partial^2 Q}{\partial x^2} = \kappa GA\left(\phi + \frac{\partial w}{\partial x}\right). \tag{A.4}$$

In the above derivation,the shear stress and strain are assumed constant across the thickness direction, which is not true in the viewpoint of a strict analysis of elasticity [26]. Therefore, κ, the shear correction factor, is introduced.

The elastodynamics of plane deformation gives the following equations of motion

$$\begin{cases} \dfrac{\partial \sigma_{xx}}{\partial x} + \dfrac{\partial \sigma_{xz}}{\partial z} = \rho z\dfrac{\partial^2 \phi}{\partial t^2}, \\ \dfrac{\partial \sigma_{xz}}{\partial x} + \dfrac{\partial \sigma_{zz}}{\partial z} = \rho\dfrac{\partial^2 w}{\partial t^2}, \end{cases} \tag{A.5}$$

where ρ is the density. For the beam model, $\sigma_{zz} = \partial\sigma_{zz}/\partial z = 0$. Multiplying z to the both sides of Eq. (A.5) and integrating over the cross-section (the $y - z$ plane), we obtain the following equation in conjunction with Eq. (A.3)

$$\begin{cases} \dfrac{\partial M}{\partial x} - Q = \rho I\dfrac{\partial^2 \phi}{\partial t^2}, \\ \dfrac{\partial Q}{\partial x} + q = \rho A\dfrac{\partial^2 w}{\partial t^2}, \end{cases} \tag{A.6}$$

where q is a prescribed transverse load per unit length. The following two equations are obtained by eliminating Q and taking the derivative on the second equation of Eq. (A.6), respectively

$$\begin{aligned} \frac{\partial^2 M}{\partial x^2} &= \rho A\frac{\partial^2 w}{\partial t^2} + \rho I\frac{\partial^3 \phi}{\partial x\partial t^2} - q, \frac{\partial^2 Q}{\partial x^2} \\ &= \rho A\frac{\partial^3 w}{\partial x\partial t^2} - \frac{\partial q}{\partial x}. \end{aligned} \tag{A.7}$$

Substituting Eq. (A.7) into Eq. (A.4), we have

$$\begin{aligned} M &= EI\frac{\partial \phi}{\partial x} + l^2\left(\rho A\frac{\partial^2 w}{\partial t^2} + \rho I\frac{\partial^3 \phi}{\partial x\partial t^2} - q\right), \\ Q &= \kappa GA\left(\phi + \frac{\partial w}{\partial x}\right) + \alpha l^2\left(\rho A\frac{\partial^3 w}{\partial x\partial t^2} - \frac{\partial q}{\partial x}\right). \end{aligned} \tag{A.8}$$

By substituting Eq. (A.8) into Eq. (A.6), the governing equations of a nonlocal Timoshenko beam are obtained as follows

$$\begin{cases} EI\dfrac{\partial^2 \phi}{\partial x^2} - \kappa GA\left(\phi + \dfrac{\partial w}{\partial x}\right) = \rho I\left(\dfrac{\partial^2 \phi}{\partial t^2} - l^2\dfrac{\partial^4 \phi}{\partial x^2\partial t^2}\right) \\ \qquad -(1-\alpha)l^2\left(\rho A\dfrac{\partial^3 w}{\partial x\partial t^2} - \dfrac{\partial q}{\partial x}\right), \\ \kappa GA\left(\dfrac{\partial \phi}{\partial x} + \dfrac{\partial^2 w}{\partial x^2}\right) + \alpha l^2\left(\rho A\dfrac{\partial^4 w}{\partial x^2\partial t^2} - \dfrac{\partial^2 q}{\partial x^2}\right) + q = \rho A\dfrac{\partial^2 w}{\partial t^2}. \end{cases} \tag{A.9}$$

For free vibration, i.e., $q = \partial q/\partial x = \partial^2 q/\partial x^2 = 0$, Eq. (A.9) is reduced to Eq. (1).

Appendix B. Proof of *a* and *b* being positive

When $\alpha = 0$, b as given in Eq. (8) becomes the following

$$\begin{aligned} b &= (1 - R_2R_3\omega^2)\omega^2 + R_1(R_2\omega^2 - R_1) + R_1(R_1 + R_3\omega^2) \\ &= [1 + R_1(R_2 + R_3) - R_2R_3\omega^2]\omega^2. \end{aligned} \tag{B.1}$$

When $\alpha = 1$, b now becomes the following

$$\begin{aligned} b &= (1 - R_2R_3\omega^2)\omega^2 + (R_1 - R_3\omega^2)(R_2\omega^2 - R_1) + R_1^2 \\ &= [1 + R_1(R_2 + R_3) - 2R_2R_3\omega^2]\omega^2. \end{aligned} \tag{B.2}$$

In conjunction with Eqs. (B.1) and (B.2), the sufficient and necessary condition for $b > 0$ is $2\omega^2 < [1 + R_1(R_2 + R_3)]/(R_2R_3) = 1/(R_2R_3) + R_1/R_3 + R_1/R_2$. As discussed in Section 2 and proved by Lei et al. [11], $\omega^2 < 1/(R_2R_3)$ and $\omega^2 < R_1/R_3$ because of the presence of two cut-off frequencies, which leads to $2\omega^2 < 1/(R_2R_3) + R_1/R_3 < 1/(R_2R_3) + R_1/R_3 + R_1/R_2$ and the proof of $b > 0$ is done. Similarly, because $\omega^2 < 1/(R_2R_3)$ and $\omega^2 < R_1/R_3$, it is obvious that $a = (1 - R_2R_3\omega^2)(R_1 - \alpha R_3\omega^2) > 0$.

Appendix C. The nonlocal Euler–Bernoulli beam theory and its eigenfrequency solution

The nonlocal Euler–Bernoulli beam theory gives the following governing equation [22]:

$$EI\frac{\partial^4 w}{\partial x^4} + \rho A\left(\frac{\partial^2 w}{\partial t^2} - l^2\frac{\partial^4 w}{\partial x^2\partial t^2}\right) = 0. \tag{C.1}$$

With the same nondimensionalization scheme as given in Eq. (2), the above equation now becomes the following

$$\frac{\partial^4 W}{\partial \xi^4} + \frac{\partial^2 W}{\partial \tau^2} - R_3\frac{\partial^4 W}{\partial \xi^2\partial \tau^2} = 0. \tag{C.2}$$

Again, by assuming $W(\xi, \tau) = Y(\xi)e^{i\omega\tau}$ and substituting it into the above equation, the following equation is obtained

$$\frac{\partial^4 Y}{\partial \xi^4} + R_3\omega^2\frac{\partial^2 Y}{\partial \xi^2} - \omega^2 Y = 0. \tag{C.3}$$

Y is with the following solution form:

$$Y(\xi) = C_1\cosh(\beta_1\xi) + C_2\sinh(\beta_1\xi) + C_3\cos(\beta_2\xi) + C_4\sin(\beta_2\xi), \tag{C.4}$$

where β_1 and β_2 are defined as follows:

$$\beta_1 = \frac{-R_3\omega^2 + \sqrt{R_3^2\omega^4 + 4\omega^2}}{2},$$
$$\beta_2 = \frac{R_3\omega^2 + \sqrt{R_3^2\omega^4 + 4\omega^2}}{2}. \tag{C.5}$$

The bending moment M and shear force Q are given as follows [22]:

$$M = -EI\frac{\partial^2 w}{\partial x^2} + \rho Al^2\frac{\partial^2 w}{\partial t^2} = -\frac{EI\omega^2}{L}\left(\frac{\partial^2 Y}{\partial \xi^2} + R_3\omega^2 Y\right),$$
$$Q = -EI\frac{\partial^3 w}{\partial x^2} + \rho Al^2\frac{\partial^3 w}{\partial x\partial t^2} = -\frac{EI\omega^2}{L}\left(\frac{\partial^3 Y}{\partial \xi^3} + R_3\omega^2\frac{\partial Y}{\partial \xi}\right). \tag{C.6}$$

In conjunction with Eq. (C.6), the following boundary conditions hold for a hinged–hinged beam

$$Y(0) = 0, \quad \frac{\partial^2 Y}{\partial \xi^2}(0) + R_3\omega^2 Y(0) = 0, \quad Y(1) = 0,$$
$$\frac{\partial^2 Y}{\partial \xi^2}(1) + R_3\omega^2 Y(1) = 0. \tag{C.7}$$

By substituting Eq. (C.4) into the above boundary conditions, the nth eigenfrequency of a hinged–hinged beam (ω_n) can be analytically derived as follows

$$\omega_n = \frac{n^2\pi^2}{\sqrt{1 + n^2\pi^2 R_3}}. \tag{C.8}$$

For the clamped–clamped beam, the following boundary conditions hold

$$Y(0) = 0, \quad \frac{\partial Y}{\partial \xi}(0) = 0, \quad Y(1) = 0, \quad \frac{\partial Y}{\partial \xi}(1) = 0. \tag{C.9}$$

By substituting Eq. (C.4) into Eq. (C.9), the following eigenvalue problem is formulated to numerically compute ω_n.

$$\begin{vmatrix} 1 & 0 & 1 & 0 \\ 0 & \beta_1 & 0 & \beta_2 \\ \cosh\beta_1 & \sinh\beta_1 & \cos\beta_2 & \sin\beta_2 \\ \beta_1\sinh\beta_1 & \beta_1\cosh\beta_1 & -\beta_2\sin\beta_2 & \beta_2\cos\beta_2 \end{vmatrix} = 0. \tag{C.10}$$

In conjunction with Eq. (C.5), the following boundary conditions hold for a cantilever beam

$$Y(0) = 0, \quad \frac{\partial Y}{\partial \xi}(0) = 0, \quad \frac{\partial^2 Y}{\partial \xi^2}(1) + R_3\omega^2 Y(1) = 0,$$
$$\frac{\partial^3 Y}{\partial \xi^3}(1) + R_3\omega^2\frac{\partial Y}{\partial \xi}(1) = 0. \tag{C.11}$$

Substituting Eq. (C.4) into Eq. (C.11) leads to the following eigenvalue problem for a cantilever beam

$$\begin{vmatrix} 1 & 0 & 1 & 0 \\ 0 & \beta_1 & 0 & \beta_2 \\ f_1\cosh\beta_1 & f_1\sinh\beta_1 & f_2\cos\beta_2 & f_2\sin\beta_2 \\ \beta_1 f_1\sinh\beta_1 & \beta_1 f_1\cosh\beta_1 & -\beta_2 f_2\sin\beta_2 & \beta_2 f_2\cos\beta_2 \end{vmatrix} = 0, \tag{C.12}$$

where f_1 and f_2 are defined as $f_1 = \beta_1^2 + R_3\omega^2$ and $f_2 = -\beta_2^2 + R_3\omega^2$, respectively.

References

[1] Timoshenko SP. On the correction for shear of the differential equation for the transverse vibrations of prismatic bars. Phil Mag 1921;41:744–6.
[2] Timoshenko SP. On the transverse vibrations of bars of uniform cross section. Phil Mag 1922;43:125–31.
[3] Traill-Nash R-W, Collar AR. The effects of shear flexibility and rotatory inertia on the bending vibrations of beams. Q J Mech Appl Math 1953;6:186–222.
[4] Downs B. Transverse vibration of a uniform, simply supported Timoshenko beam without transverse deflection. J Appl Mech 1976;43:671–4.
[5] Abbas B, Thomas J. The second frequency spectrum of Timoshenko beams. J Sound Vibr 1977;51:123–37.
[6] Bhashymam GR, Prathap G. The second frequency spectrum of Timoshenko beams. J Sound Vibr 1981;76:407–20.
[7] Levinson M, Cooke DW. On the two frequency spectra of Timoshenko beams. J Sound Vibr 1982;84:319–26.
[8] Chan, Wang, So, Reid SR. Superposed standing waves in a Timoshenko beam. Proc R Soc Lond A 2002;458:83–108.
[9] Stephen NG. The second spectrum of Timoshenko beam theory-further assessment. J Sound Vibr 2006;292:372–89.
[10] Mindlin RD. Thickness-shear and flexural vibrations of crystal plates. J Appl Phys 1951;22:316–23.
[11] Lei, Adhikari S, Friswell MI. Vibration of nonlocal Kelvin–Voigt viscoelastic damped Timoshenko beams. Int J Eng Sci 2013;66–67:1–13.
[12] Eringen AC. On differential equations of nonlocal elasticity and solutions of screw dislocation and surface waves. J Appl Phys 1983;54:4703–10.
[13] McFarland AC, Colton JS. Role of material microstructure in plate stiffness with relevance to microcantilever sensors. J Micromech Microeng 2005;15:1060–7.
[14] Maranganti R, Sharma P. Length scales at which classical elasticity breaks down for various materials. Phys Rev Lett 2007;98:195504.
[15] Love AEH. The mathematical theory of elasticity. Dover Publications 1927.
[16] Peddieson J, Buchanan GR, McNitt RP. Application of nonlocal continuum models to nanotechnology. Int J Engr Sci 2003;41:305–12.
[17] Li, Wang. Vibrational modes of Timoshenko beams at small scales. Appl Phys Lett 2009;94:101903.
[18] Abbasion S, Rafsanjani A, Avazmohammadi R, Farshidianfar A. Free vibrational of microscaled Timoshenko beams at small scales. Appl Phys Lett 2009;95:143122.
[19] Wang, Zhang, He. Vibration of nonlocal Timoshenko beams. Nanotechnology 2007;18:105401.
[20] Wang, Zhang, Ramesh S, Kitopornchai S. Buckling analysis of micro- and nano-rods/tubes based on nonlocal Timoshenko beam theory. J Phys D: Appl Phys 2006;39:3904–9.
[21] Zhang, Challamel N, Wang. Eringen's small length scale coefficient for buckling of nonlocal Timoshenko beam based on microstructured beam model. J Appl Phys 2013;114:114902.
[22] Lu, Lee, Lu, Zhang. Dynamic properties of flexural beams using a nonlocal elasticity model. J Appl Phys 2006;99:0753510.
[23] Xu. Free transverse vibrations of nano-to-micron scale beams. Proc R Soc Lond A 2006;462:2977–95.
[24] Wang. Wave propagation in carbon nanotubes via nonlocal continuum mechanics. J Appl Phys 2005;98:124301.
[25] Wang, Hu. Flexural wave propagation in single-walled carbon nanotubes. Phys Rev B 2005;71:195412.
[26] Cowper GR. The shear coefficient in Timoshenko's beam theory. J Appl Mech 1966;33:335–40.
[27] Shi, Shen, Peng, Li. Frequency equation and resonant frequencies of free-free Timoshenko beams with unequal end mass. Int J Mech Sci 2016;115–116:406–15.
[28] Shaw S. High frequency vibration of a rectangular micropolar beam: a dynamical analysis. Int J Mech Sci 2016;108–109:83–9.
[29] Chang, Craig RR. Normal modes of uniform beams. J Eng Mech 1969;195:1027–31.
[30] Dillard T, Forest S, Ienny P. Micromorphic continuum modelling of the deformation and fracture behavior of nickel foams. Eur J Mech A/Solids 2006;25:526–49.
[31] Press WH, Flannery BP, Teukolsky SA, Vettering WT. Numerical recipes. Cambridge University Press; 1986.
[32] Zhang, Zhuo, Zhao. Determining the effects of surface elasticity and surface stress by measuring the shifts of resonant frequencies. Proc R Soc Lond A 2013;469:20130449.
[33] Challamel N, Zhang, Wang, Reddy JN, Wang, Michelitsch T, et al. On non-conservativeness of Eringen's nonlocal elasticity in beam mechanics: correction from discrete-based approach. Arch Appl Mech 2014;84:1275–92.
[34] Reddy JN, El-Borgi S. Eringen's nonlocal theories of beam accounting for moderate rotations. Int J Eng Sci 2014;82:159–77.
[35] Fernandez-Saez J, Zaera R, Loya JA, Reddy JN. Bending of Euler–Bernoulli beams using Eringen's integral formulation: a paradox resolved. Int J Eng Sci 2016;99:107–16.
[36] Romano G, Barretta R, Diaco M, de Sciarra FM. Constitutive boundary conditions and paradoxes in nonlocal elastic beams. Int J Mech Sci 2017;121:151–6.
[37] Zhang, Liu, Xie. Free transverse vibration of double-walled carbon nanotubes using a theory of nonlocal elasticity. Phys Rev B 2005;71:195404.
[38] Sudak LJ. Column buckling of multiwalled carbon nanotubes using nonlocal continuum mechanics. J Appl Phys 2003;94:7281–7.
[39] Liang, Han. Prediction of nonlocal scales parameter for carbon nanotubes. Sci Chin Phys Mech Astron 2012;55:1670–8.
[40] Zhang, Wang, Challamel N, Elishakoff I. Obtaining Eringen's length scale coefficient for vibrating nonlocal beams via continualization method. J Sound Vibr 2014;33:4977–90.
[41] Mindlin RD. Elasticity, piezoelectricity and crystal dynamics. J Elast 1972;2:217–82.